High Resolution Numerical Simulation for corner-turning in LX-17

†C. Wang, *X.Q. Liu

State Key Lab of Explosion Science and Technology, Beijing Institute of Technology, Beijing, 100081, China

*Presenting author: 3120100070@bit.edu.cn †Corresponding author: wangcheng@bit.edu.cn

Abstract

In this paper, Combined with the third-order TVD Runge-Kutta method, we develop a parallel solver using the fifth-order high-resolution weighted essentially non-oscillatory (WENO) finite difference scheme to simulate detonation diffraction for three-dimensional condensed explosives. Using the explosive LX-17, abrupt corner turning of detonation was investigated as the detonation moved from a near-ideal cylinder of small radius suddenly into a cylinder of large radius. The numerical simulation results revealed the restrictive relationships among the pressure, the density and the reaction progress in the failure regions around the corner. As a result, the detonation cannot turn the corner and subsequently fails, but the shock wave continues to propagate in the unreacted explosive, leaving behind a dead zone. Previously, we have used the PBX-9404 explosive to simulation the detonation diffraction. Comparing with that, the inert explosive LX-17 has the longer distance to detonation along the inner wall. It demonstrated that a larger field of the dead zone can be generated, and it may not close.

Keywords: Condensed explosives; Numerical simulation; WENO; High resolution; Corner-Turning; Dead zone

Introduction

The ability of a detonation wave to continue to propagate after it encounters an abrupt or a more gradual geometry change is very important to understand in practical explosive charge design. The corner leads the detonation wave to curve and spread to the side along the inner wall, and the reaction zone may decouple and lag behind the shock. If extinction occurs, the lead shock degrades into a weak shock followed by a fast flame. The dead zone represents a loss of available energy in the system to do work and must be computed accurately.

Numerous experimental and numerical studies have been performed to study corner turning phenomena. Souers et al. [2004] have performed a series of highly-instrumented experiments examining corner-turning of detonation, and they used pulsed X-rays to observe the dead zones in ambient detonating LX-17 with the breakout on the edges measured by streak camera. Cox and Campbell studied the ability of PBX 9502 to turn corners using a long, cylindrical straight section that suddenly changes into a much wider cylinder, which has a slice taken out of one side [Cox and Campbell (1981)]. They concluded that the explosive had a 17mm corner turning radius, and that the explosive inside this radius did not detonate. The most detailed experiments of TATB corner turning and dead zone formation are those fired using proton radiography at Los Alamos National Laboratory[Ferm et al. (2002); Mader et al. (2002)]. The greater penetrating power of high energy protons compared to X-rays allows finer structures of the dead zones to be observed. Kapila [Kapila et al. (2007) simulated the process of detonation diffraction of the explosive LX-17 with different corners by second-order accurate capture scheme to research the changes of the explosive state at the corner wall under the influence of detonation diffraction around the corner and observed the initiation process along the inner wall to be similar to the shock-initiation under low-pressure. Tarver[2010] modeled the hydrodynamics of double corner turning and shock desensitization in two dimensions using the Ignition and Growth LX-17 detonation reactive flow model. They compared the calculated arrival times and axial free surface velocity histories of the top aluminum plates with the experimental measurements, well in agreement. In recent years, Yang G. [Yang et al. (2013)] used the smoothed particle hydrodynamics (SPH) method combined with ignition and growth model to give good prediction for the von Neumann spike state of detonation in condensed explosives. The smoothed particle hydrodynamics (SPH) method is more and more widely applied to investigate the detonation phenomena, e.g. [Yang et al. (2011); Hu et al. (2014)].

In this paper, the process of corner-turning of the double cylinder geometries in LX-17 are numerically simulated by high resolution numerical scheme. Fifth-order WENO scheme [Jiang and

Shu (1996)] and third-order TVD Runge-Kutta method are employed to discretize Euler equations with chemical reaction source, and parallel high resolution code is developed. The code was used to stimulate the process of detonation diffraction at the corner. Respectively, the change rules of pressure, density and reaction rate in the low-pressure region and the inner wall region will be investigated, and the corner effect on the detonation wave propagation will be discussed.

1. Governing equations

The detonation process is very short, so the transport effect of viscosity, heat conduction and diffusion can be neglected in the detonation process. The non-stationary compressible Euler equations can be used as the fluid dynamics governing equations. In the form as follows

$$\mathbf{U}_{t} + \mathbf{F}(\mathbf{U})_{y} + \mathbf{G}(\mathbf{U})_{y} + \mathbf{H}(\mathbf{U})_{z} = \mathbf{S}(\mathbf{U})$$
 (1)

Where the conserved variable vector U, the flux vectors F, G and H as well as the source term S are given, respectively, by

$$\mathbf{U} = (\rho, \rho u, \rho v, \rho w, \rho E, \rho \lambda)^{\mathrm{T}}$$
(2)

$$\mathbf{F}(\mathbf{U}) = \left(\rho u, \rho u^2 + p, \rho uv, \rho uw, \rho u(E + p/\rho), \rho u\lambda\right)^{\mathrm{T}}$$
(3)

$$\mathbf{G}(\mathbf{U}) = (\rho v, \rho v u, \rho v^2 + p, \rho v w, \rho v (E + p/\rho), \rho v \lambda)^{\mathrm{T}}$$
(4)

$$\mathbf{H}(\mathbf{U}) = (\rho v, \rho w u, \rho w v, \rho w^2 + p, \rho w (E + p/\rho), \rho w \lambda)^{\mathrm{T}}$$
(5)

$$\mathbf{S}(\mathbf{U}) = (0, 0, 0, 0, 0, 0, \rho \lambda)^{\mathrm{T}}$$
(6)

$$E = e + (1 - \lambda)q + \frac{1}{2}(u^2 + v^2)$$
 (7)

Here u, v, w are the Cartesian component of the particle velocity in the x, y, z directions. Respectively, ρ is density, p is pressure, E is total energy per unit volume, e is internal energy, λ is reaction rate variable.

2. Equations of state and reaction rate

The unreacted explosive and the reaction products are both described by the JWL equation of state, but their parameter values are different. For LX-17 explosive, the specific parameter values of equation of state are shown in Table 1 [Zhang and Chen (1991)].

$$p = A \exp(-R_1 V) + B \exp(-R_2 V) + \frac{\omega}{V} C_{\nu} T$$

$$e = \frac{A}{\rho_0 R_1} \exp(-R_1 V) + \frac{B}{\rho_0 R_2} \exp(-R_2 V) + \frac{C_{\nu} T}{\rho_0}$$

$$V = \upsilon / \upsilon_0$$
(8)

Table 1. EOS data for the explosive LX-17

JWL parameters	Unreacted	Products	
$A(10^2$ GPa)	77.81	6.547	
$B(10^2\text{GPa})$	-1.5031	0.7124	
$C\dot{v}(10^2\text{GPa/K})$	$2.487 \times 10-5$	$1.0 \times 10 - 5$	
R_1	11.3	4.45	
$egin{array}{c} R_1 \ R_2 \end{array}$	1.13	1.2	
ω	0.8939	0.38	
$\rho_0(g/cm^3)$	1.895	1.895	

Respectively, v is the specific volume, and v_0 is the specific volume at the initial moment. A, B, R_1 , R_2 , C_v and ω are constants, and T is temperature.

The most commonly used chemical reaction rate model of condensed explosives is the ignition and growth reaction rate model proposed by Lee and Tarver. For LX-17 explosive, the specific parameter values of the chemical reaction rate equation are shown in Table 2 [Zhang and Chen (1991)].

$$\frac{d\lambda}{dt} = I(1-\lambda)^{b} (\rho / \rho_{0} - 1 - a)^{x} + G_{1}(1-\lambda)^{c} \lambda^{d} p^{y} + G_{2}(1-\lambda)^{e} \lambda^{g} p^{z}$$
(9)

Here I, G_1 , G_2 , b, a, x, c, d, y, e, g and z are constants.

Table 2. Rate data for the explosive LX-17

Parameters	Value
<i>I</i> (μsec ⁻¹)	4.0×10^6
$G_1(\mu \text{sec}^{-1}(10^2\text{GPa})^{-z})$	0.6
$G_2(\mu \text{sec}^{-1}(102\text{GPa})^{-z})$	400
b	0.667
a	0.22
X	7.0
c	0.667
d	0.111
y	1.0
e	0.333
g	1.0
Z	3.0

3. The numerical method

In this paper, WENO finite difference scheme is employed to discretize Euler equations with chemical reaction source in space. The semi-discrete scheme is as follows:

$$\left(\frac{\partial \mathbf{U}}{\partial t}\right)_{i,j,k} = -\frac{\left(\tilde{\mathbf{F}}_{i+1/2,j,k} - \tilde{\mathbf{F}}_{i-1/2,j,k}\right)}{\Delta x} - \frac{\left(\tilde{\mathbf{G}}_{i,j+1/2,k} - \tilde{\mathbf{G}}_{i,j-1/2,k}\right)}{\Delta y} - \frac{\left(\tilde{\mathbf{H}}_{i,j,k+1/2} - \tilde{\mathbf{H}}_{i,j,k-1/2}\right)}{\Delta z} + \mathbf{S}_{i,j,k} \tag{10}$$

Third-order TVD Runge-Kutta scheme is employed for temporal discretization.

$$\begin{cases}
\mathbf{U}_{i,j,k}^{(1)} = \mathbf{U}_{i,j,k}^{n} + \Delta t L(\mathbf{U}_{i,j,k}^{n}) \\
\mathbf{U}_{i,j,k}^{(2)} = \frac{3}{4} \mathbf{U}_{i,j,k}^{n} + \frac{1}{4} \mathbf{U}_{i,j,k}^{(1)} + \frac{1}{4} \Delta t L(\mathbf{U}_{i,j,k}^{(1)}) \\
\mathbf{U}_{i,j,k}^{n+1} = \frac{1}{3} \mathbf{U}_{i,j,k}^{n} + \frac{2}{3} \mathbf{U}_{i,j,k}^{(2)} + \frac{2}{3} \Delta t L(\mathbf{U}_{i,j,k}^{(2)})
\end{cases}$$
(11)

4. Results and discussion

The explosive LX-17 is selected as an example, and the model geometry size is shown in figure 1. There is the inflow boundary conditions on the left of the small radius cylinder and all other boundaries are set wall boundary conditions. We take the mesh size Δ =0.1(mm), and the explosive is initiated by C-J (Chapman-Jouguet) condition within 0.5mm distance on the left of the small radius cylinder.

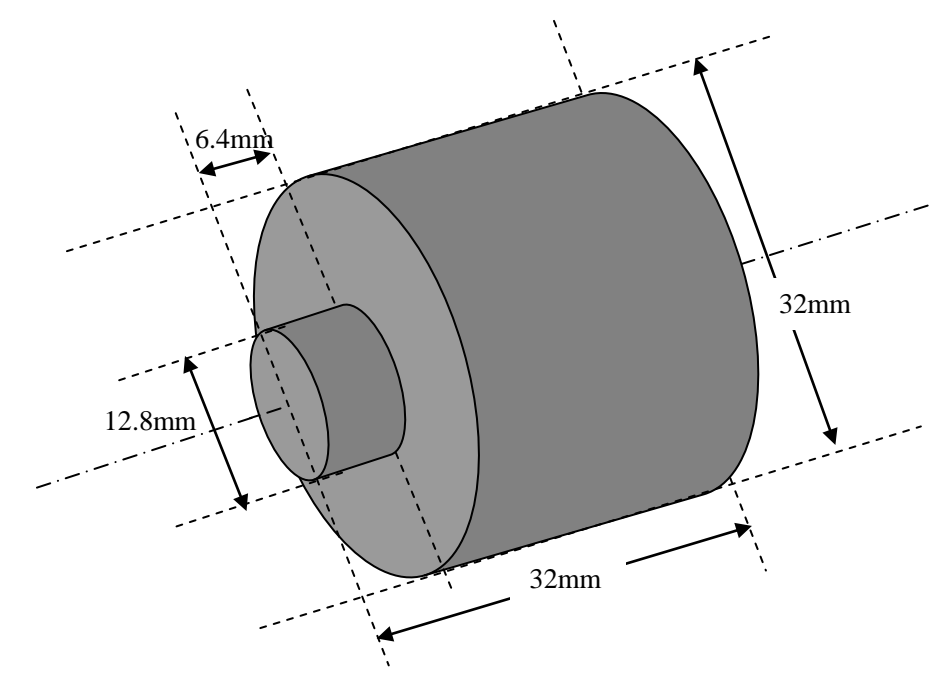
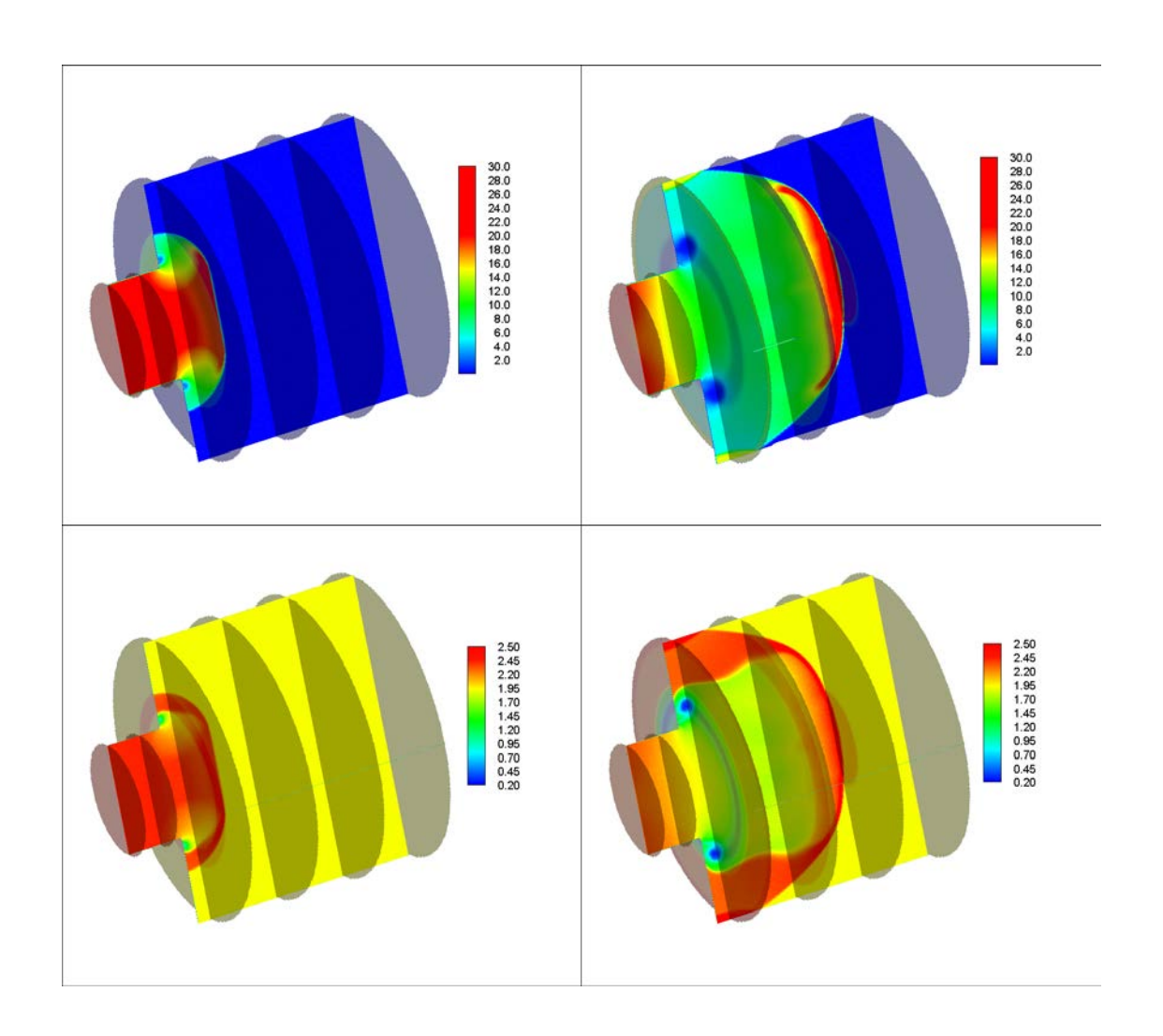


Fig. 1. Schematic for the double-cylinder corner-turning model



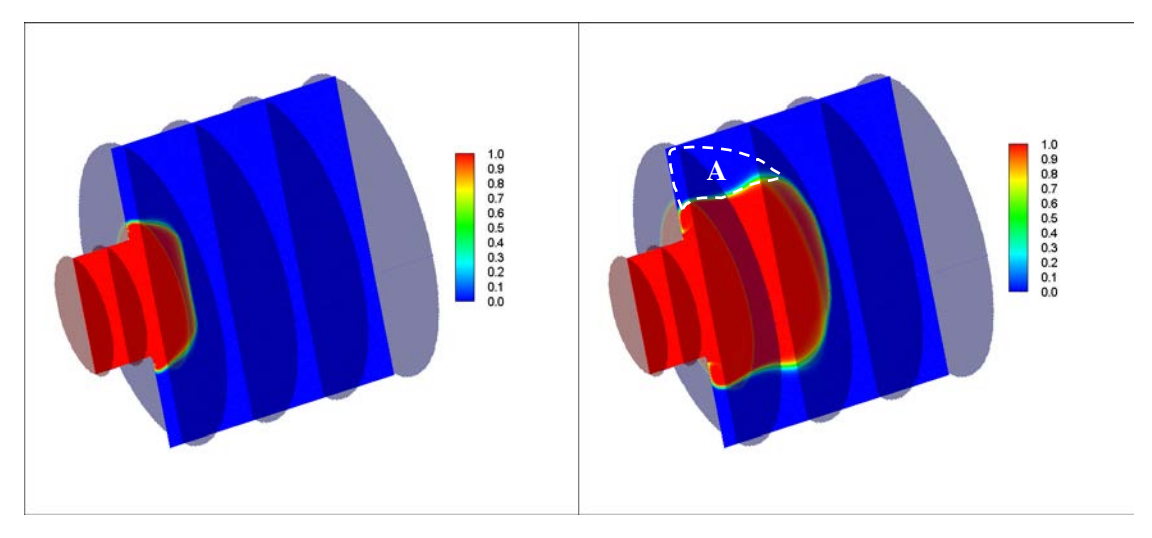


Fig. 2. Contours of pressure (top), density (middle) and the reaction rate (bottom) of the double-cylinder corner-turning at 1.65μs (left), 3.3μs (right)

Previously, we have obtained The propagating state of detonation wave around the corner is generally determined by two factors in the other paper. One is the transverse shock wave along the inner wall downwards, and the other is the extending curved detonation wave. In this model, when the detonation wave reaches the corner position, the time span is 0.97µs. From figure 2, because of the effect of corner turning influence, the expansion generated there is felt by the lead shock.

At 1.65µs, the influencing regions domain centred around the corner, and the low-pressure region, low-density region have appearanced. Comparing the contour of the reaction rate with the contours of the pressure and the density, we can find that the shock wave continues to propagate in the unreacted explosive, leaving behind unreacted explosive. The dead zone, which is a region of unreacted explosive, generally forms around the right-angle turn. At this moment, the dead zone appears primarily behind the lead shock wave. Then the factor of the transverse shock wave along the inner wall downwards plays a leading role, and the extending curved detonation wave have just extended alightly. In the center position of the model section, there is still the steady detonation wave propagating forward along the central axis of the model. At 3.3µs, as the detonation wave propagates forward and extends to the sides of the head shock wave, the low-pressure region and the low-density region have become increasingly large. Along the inner wall, the lead shock wave has reached the edges of the cylinder, and the reflection can be seen. However, lots of unreacted explosive is left behind the lead shock wave. It demonstrated the failure exits, and the failure/dead zone has been shown in the figure 1 as the region A. It looks like a turnip shape which has a good consistent with the experimental results[Souers et al. (2006)].

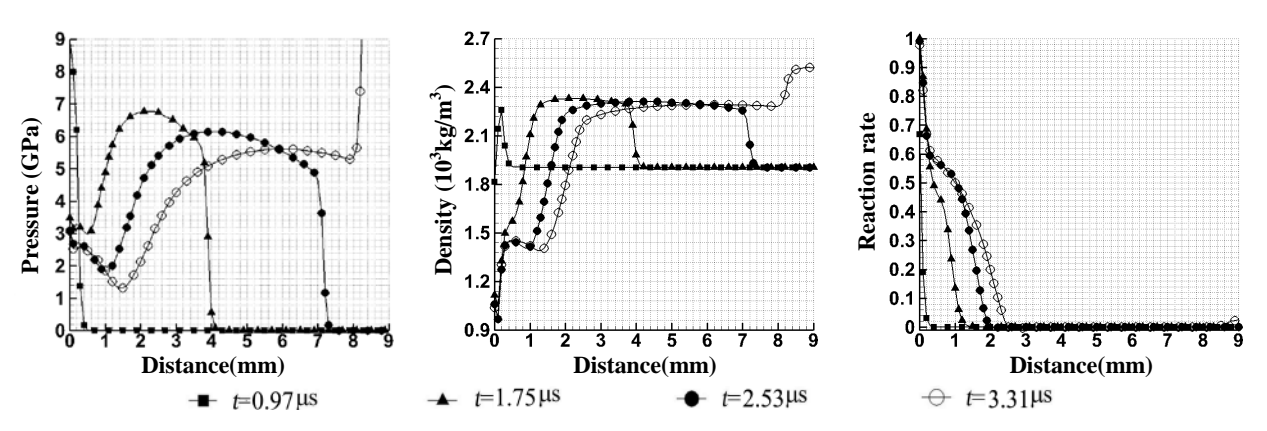


Fig. 3. Plots of pressure, density and the reaction rate along the inner wall at different moments

As showed the plot of pressure in figure 3, at 0.97µs, the detonation wave just arrived at the corner position, and the transverse shock wave causes pressure changes only within 0.5mm along the inner wall. The maximum is 9Gpa and rapidly decreased to 0. The lead shock wave propagates 4.1mm and 7.2mm along the inner wall at 1.75µs and 2.53µs respectively. At 3.31µs, the lead shock wave has reached the edges of the cylinder. The low-pressure region can be clearly shown by the plot of pressure at different moment. And again, the low-density region can be seen from the plot of density, and we can find, in the low-density region, the density has fallen below the initial density. From the plot of the reaction rate, at 3.31µs, we can see that the reaction progress will decline to 0 directly, which suggests only slight retonation generating. With time lapsing, the re-initiation is failure. In the next moment, the extending curved detonation wave reachs the inner wall to re-initiate, otherwise it is detonation failure along the inner wall.

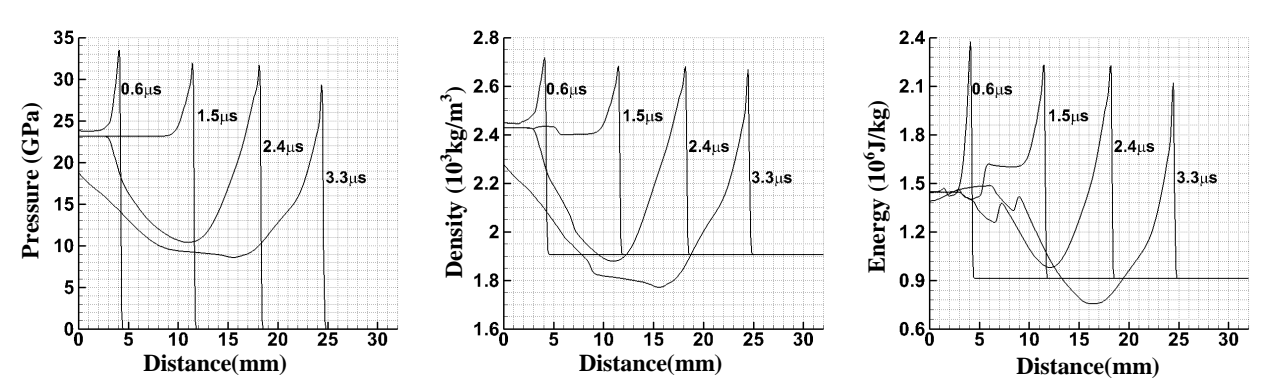


Fig. 4. Plots of pressure, density and tatal energy along the the central axis of the model at different moments

The figure 4 gives the corner-turning influence on the pressure, density and energy in the position of the central axis. After the detonation wave has reached the corner, the detonation wave in the axis position has little effect, and it still keep steady detonation to propagate forward. At 2.4µs and 3.3µs, because of expansion, the troughs appear behind the detonation wave. The trailing expansion region shows some effects of the signals of expansion emanating from the corner. By contrast, the evolution along the wall is more complex, as discussed in detail above.

Conclusions

In this paper, Fifth-order WENO scheme and third-order TVD Runge-Kutta method are employed to investigate the process of the corner turning of LX-17. The parallel high resolution code is developed. By calculation and detailed analysis for the corner-turning of the double cylinder geometries, we can obtain the following conclusions:

- (1) As showed in the example, using the LX-17 explosive, the detonation failure happens along the inner wall, and there is no re-initiation subsequently within a radius of 9.6mm. The transverse shock wave plays little direct role for initiation explosive which swept by the lead shock wave. In addition, the extending curved detonation wave needs a long time to reach the inner wall. Because of the two factors, there is a great proportion of unreacted explosive remained, forming a large area of dead zone.
- (2) The low-pressure, low-density regions are formed in the vicinity of the corner, in which the explosive will react slowly in the subsequent steps, but the released energy cannot support the transverse shock wave propagation forward to re-initiate explosive.

References

- Souers, P. C., Andreski, H. G., Cook III, C. F., Garza, R., Pastrone, R., Phillips, D., Roeske, F., Vitello, P., Molitoris, J. D. (2004) LX-17 Corner Turning, *Propellants, Explos., Pyrotech* **29**, 359-367.
- Cox, M. and Campbell, A. W. (1981) *Corner-turning in TATB* (No. LA-UR-81-739; CONF-810602-13). Los Alamos Scientific Lab., NM (USA).
- Ferm, E. N., Morris, C. L., Quintana, J. P., Pazuchanic, P., Stacy, H., Zumbro, J. D., Hogan, G. and King, N. (2002, July) Proton radiography examination of unburned regions in PBX 9502 corner turning experiments. *In AIP Conference Proceedings* (No. 2, pp. 966-972). IOP INSTITUTE OF PHYSICS PUBLISHING LTD.
- Mader, C. L., Zumbro, J. D., Ferm, E. N., Gittings, M. and Weaver. R. (2002) Proton radiographic and numerical modeling of colliding, diverging PBX 9502 Detonations. Paper presented at the 12th International Detonation Symposium, August 11–16, San Diego, CA.
- Kapila, A. K., Schwendeman, D. W., Bdzil, J. B. and Henshaw, W. D. (2007) A study of detonation diffraction in the ignition-and-growth model. Combust. Theor. Model. 11(5): 781-822.
- Tarver, C. M. (2010) Corner turning and shock desensitization experiments plus numerical modeling of detonation waves in the triaminotrinitrobenzene based explosive LX-17. *The Journal of Physical Chemistry A* **114**(8): 2727-2736.
- Yang, G., Fu, Y., Hu, D. and Han, X. (2013). Feasibility analysis of SPH method in the simulation of condensed explosives detonation with ignition and growth model. *Computers & Fluids* 88: 51-59.
- Yang, G., Han, X. and Hu, D. (2011). Computer simulation of two-dimensional linear shaped charge jet using smoothed particle hydrodynamics. *Engineering Computations* **28**(1): 58-75.
- Hu, D., Liu, C. H., Xiao, Y. H. and Han, X. (2014). Analysis of explosion in concrete by axisymmetric FE-SPH adaptive coupling method. *Engineering Computations* **31**(4): 758-774.
- Jiang, G. S. and Shu, C. W. (1996). Efficient implementation of weighted ENO schemes. *J. Comput. Phys* **126**(1): 202-228.
- Zhang, G. R. and Chen, D. N. (1991). Dynamics of Condensed Explosives Initiation Detonation. National Defense Industry Press, Beijing.
- Souers, P. C., Andreski, H. G., Batteux, J., Bratton, B., Cabacungan, C., Cook, C. F., ... and Vitello, P. (2006) Dead Zones in LX 17 and PBX 9502. *Propellants, Explosives, Pyrotechnics* **31**(2), 89-97.